

The Cryogenic Test Bed Experiments
Cryogenic Heat Pipe Flight Experiment CRYOHP (STS-53)
Cryogenic Two Phase Flight Experiment CRYOTP (STS-62)
Cryogenic Flexible Diode Flight Experiment CRYOFD

Lee Thienel
Jackson and Tull
Albuquerque, NM

Chuck Stouffer
OAO Corporation
Lanham, MD

ABSTRACT

This paper presents an overview of the Cryogenic Test Bed (CTB) experiments including experiment results, integration techniques used, and lessons learned during integration, test and flight phases of the Cryogenic Heat Pipe Flight Experiment (STS-53) and the Cryogenic Two Phase Flight Experiment (OAST-2, STS-62). We will also discuss the Cryogenic Flexible Diode Heat Pipe (CRYOFD) experiment which will fly in the 1996/97 time frame and the fourth flight of the CTB which will fly in the 1997/98 time frame. The two missions tested two oxygen axially grooved heat pipes, a nitrogen fibrous wick heat pipe and a 2-methylpentane phase change material thermal storage unit. Techniques were found for solving problems with vibration from the cryo-coolers transmitted through the compressors and the cold heads, and mounting the heat pipe without introducing parasitic heat leaks. A thermally conductive interface material was selected that would meet the requirements and perform over the temperature range of 55 to 300 K. Problems are discussed with the bi-metallic thermostats used for heater circuit protection and the S-Glass suspension straps originally used to secure the BETSU PCM in the CRYOTP mission. Flight results will be compared to 1-g test results and differences will be discussed.

INTRODUCTION

An objective of the Cryogenic Heat Pipe Flight Experiment (CRYOHP) was to develop a reusable Cryogenic Test Bed (CTB) for use in joint NASA/USAF flight experiments. In the process of fulfilling this objective several techniques were developed to integrate the test articles with the experiment and lessons were learned from efforts that did not produce the expected/desired results. The Cryogenic Two Phase Flight Experiment (CRYOTP) was the first re-flight of the CTB. More was learned and is still being learned about the CTB and implementation of the various cryogenic experiments after the second flight and as preparations are being started for the third flight of the CTB. The third flight will test two cryogenic flexible diode heat pipes (one charged with oxygen and the other charged with methane) and is currently planned for late 1996. The fourth flight of the CTB will test a 60 Kelvin thermal storage unit.

CTB Description

The CTB was developed for NASA's Goddard Space Flight Center (GSFC) and the USAF's Wright Laboratory. Figure 1 shows the CTB configuration and major components (this configuration shows the heat pipes flown on CRYOHP). The CTB is designed to test two cryogenic thermal devices, each on a separate cryogenic system using tactical cryogenic coolers (providing 3.5 W of cooling at 80 K each). The coolers have a Coefficient of Performance (CoP) of 25 to 30. One test article is cooled with three coolers and the other is cooled with two coolers. The Hitchhiker (HH) canister is fitted with a modified Upper End Plate (UEP) having an additional 40 Kg of thermal mass and increased surface area to allow for up to 12 hours continuous operation while maintaining the cryogenic cooler compressor bodies below 80°C with up to 320 watts of heat dissipation.

The test articles are supported by a stainless steel support structure which is thermally de-coupled from the UEP by G-10 spacers inserted in the vertical legs of the support structure. The cryogenic coolers are coupled to the test articles using vibration isolation mounts and thermal shunts to couple the multiple cryogenic coolers, provide thermal mass, and to span the vertical distance from the cold heads to the test article.

Graphite foil conductive interfaces and G-10 isolators are used throughout the experiment as necessary to either minimize the ΔT (graphite foil) or the heat flow across the interface (G-10). Individual components and assemblies were wrapped with multi-layer insulation (MLI) blankets as necessary to minimize radiation heat leaks (parasitic heat loads).

Power (for electronics and experiment heaters), command and telemetry interfaces are provided by the CTB electronics control module (CECM) and the power and control for the cryo-coolers are controlled by the power distribution box (PDB). The CRYOHP mission was a side mount experiment and four sets of HH power and signal lines were available for the CRYOHP (3 for the experiment and one for the lower end plate (LEP)). The CRYOTP mission was a bridge mount, and only three sets of power and signal lines were available.

We had to modify the PDB for the CRYOTP mission to require fewer pulse commands for experiment control. The original design had twelve pulse commands:

- CECM ON/OFF (2 commands)
- CRYO-Cooler ON/OFF (2 each for 5 coolers = 10 commands)

Only ten commands were available for the CRYOTP flight. Since it was not part of the mission plan to run both sides of the CTB at any time it would be possible to have commands that turn off two cryo-coolers (1 on each side) since both would never be on. We modified the PDB circuitry so that one command would turn off the #1 coolers on each side of the experiment and another would turn off both #2 coolers.

Each test article and its associated hardware (thermal shunt, cryo-cooler cold heads, etc.) are instrumented with 13 platinum resistance thermometers (PRTs) providing accurate temperature data over the range of 50 to ~200 K. Thermistors were used for temperature measurements in the range of 200 - 350 K.

BI-METALLIC THERMOSTATS

Shuttle safety requirements led us to a heater circuit design based on a tri-series redundant thermostat system with one thermostat on the return leg of the heater (if different set points are used on the same circuit the lowest set point is used on the return leg).

The thermostats preferred for space applications (based on our knowledge and resources) are not rated for cryogenic applications. We found that the set point of the thermostat dropped dramatically after exposure to cryogenic temperatures. This phenomenon was observed during testing with the CRYOHP experiment. Figure 2 shows data for a thermostat of the type used with a specified open on rise temperature of $58 \pm 2^\circ\text{C}$, and an original open temperature of 57.4°C . As shown in

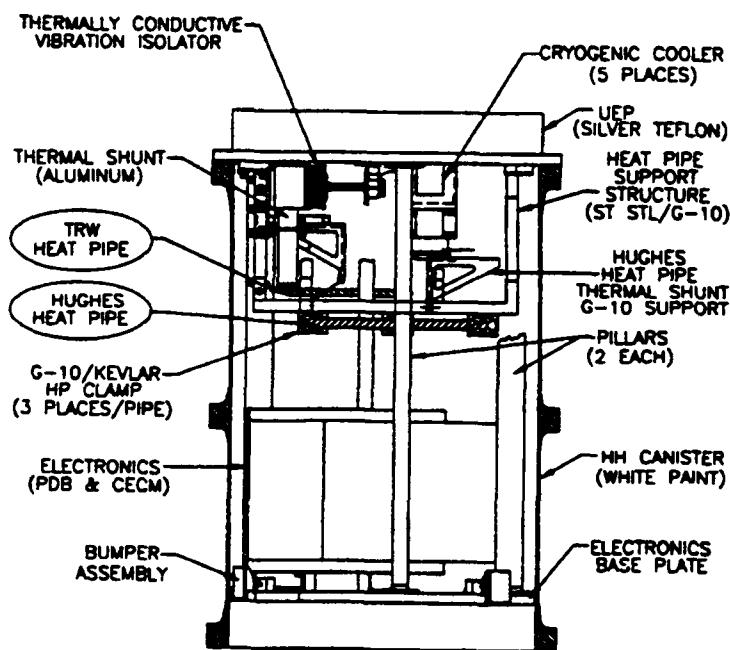


Figure 1. CTB Configuration

Figure 2, the set point moved to $\sim 3^{\circ}\text{C}$ after exposure to liquid nitrogen (LN_2) temperatures. This unit (still in its test set-up) was retested after more than 18 months of storage at room temperature. Repeated testing revealed that the unit's set point had not changed. There was some concern that, after time, the set point may start to return to its original value. If the set point drifted during storage one may have to prove that it would never rise above its original value to satisfy Space Shuttle (NSTS) safety requirements.

Less formal observations indicate that as units flown on CRYOHP were exposed to temperatures below LN_2 the set point dropped even lower. We have taken this series of thermostat to temperatures in the range of 60 K without any failures. The issue does not seem to be that a unit might fail but rather that the set point will drop to a temperature below 0°C or close enough to 0°C that it is not possible to use the experiment heaters to warm up the test articles during thermal vacuum testing. This is undesirable because it is time consuming and costly to wait for the experiment to warm up on its own in a vacuum. Some of the units that we used on the first flight had set points specified as low as 30°C and they drifted to approximately -20°C after exposure to cryogenic temperatures.

TESTING WITH HH

When the experiments were delivered to GSFC for flight as HH payloads they underwent a series of testing. The sequence of tests was the same for both the CRYOHP and CRYOTP missions.

The first test run after delivery to HH was a post ship functional. We delivered our ground support equipment (GSE) with the experiment to allow for performance of the post ship functional and any future stand alone testing that circumstances might have required. The post ship functional tests were straight forward, and no problems were encountered.

The first test run after delivery to HH was a post ship functional. We delivered our ground support equipment (GSE) with the experiment to allow for performance of the post ship functional and any future stand alone testing that circumstances might have required. The post ship functional tests were straight forward, and no problems were encountered.

The next test to be performed was an interface verification test (IVT). The purpose of this test is to perform a safe-to-mate test followed by verification of the power interface. The IVT is designed to verify that the experiment will not damage the HH avionics. We also performed a safe-to-mate test on the avionics and flight harness with the measurements being made at the LEP. The only anomaly that we found was on the LEP where two of the HH signal connectors are mislabeled.

After power interface verification the experiment was mated with the HH and the command and telemetry interfaces were verified. The only problem encountered in the IVT was on CRYOHP, there was a bad integrated circuit on the RS422 interface and only one side of the differential signals was present (the other was floating). The problem did not show up during experiment level testing because the experiment RS422 interface was tied to a commercial RS422/RS232 converter. It turned out that the converter used would still work with only one side of the differential RS422 signal. After replacing the chip, no other problems were encountered.

After the IVTs were performed for all of the experiments, the HH and the experiments were taken to the Electromagnetic Interference (EMI)/Electromagnetic Compatibility (EMC) test facility at GSFC. We experienced two problems in EMI/EMC, the first was that the coolers had high in-rush characteristics that were deemed allowable (the coolers have in-line EMI filters). The other problem we experienced was a susceptibility to conducted emissions in the range of 1-50 MHz. We ran diagnostic tests to determine the levels at which CTB became susceptible. We determined that it was unlikely that we would encounter noise at levels that would cause problems for us (the experiment was not susceptible at the STS/HH ICD levels). During both flights of the CTB we only had noise in the telemetry due to internal circuits controlling experiment heater power levels.

CRYOTP emissions were too high in a frequency range which could have interfered with the Shuttle crews intercom system (used by some crews to communicate between compartments). When Johnson Space Center (JSC) was contacted it was discovered that there was revised data for the intercom system which increased the level of noise that could be present without impacting the intercom system and the experiment met this new specification.

BRILLIANT EYES THERMAL STORAGE UNIT (BETSU)

During the flight qualification of the CRYOTP Flight Experiment the S-Glass suspension System that was used to support the BETSU canister failed under vibration. The following summary describes the BETSU design, failure event and the corrective action taken to qualify and successfully fly the experiment.

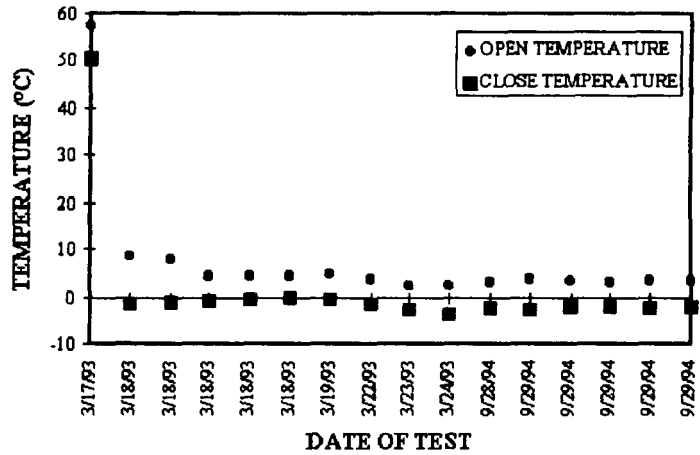


Figure 2. Thermostat Test Data

The structural configuration of the BETSU experiment consisted of an internal PCM canister suspended from the outer shell as illustrated in Figure 3. Due to the small envelope available, the cable system was designed with very short cable lengths. The system was designed using six S-Glass fixed loops; each being approximately 1" long. S-Glass material has a very small linear stretch under tension, and therefore the system was designed with a very short stroke for adjusting tension in the cable.

The experiment was tested in the HH canister at protoflight random vibration levels. The input levels and the levels observed by the BETSU due to transmissivity of the HH canister mounts are shown in Table 1. During the post vibration evaluation it was apparent the S-Glass straps had failed leaving the lacing cord back-up straps completely supporting the internal BETSU canister. A failure evaluation was performed with the BETSU unit including segmented vibration testing and inspections to determine the failure modes. During this evaluation a microscopic inspection of the fractured straps revealed two failure modes for these straps, wearing on the internal radius and stress cracks in the radius. A study was performed to evaluate alternative strap types and/or materials that could be used for this application. The following parameters were used as a baseline for the study:

- Thermal conductance
- Envelope constraints
- Short length of straps that the BETSU can accommodate
- Tension adjustment 15 mm (0.6") maximum
- No linear take-up mechanism to accommodate cable stretch

The study included fabrication and testing of materials such as, s-glass, aramid (braid and weave), stainless steel and titanium wire.

Aramid (braid and weave) was eliminated as a option due to its stretch under tension which could not be accommodated in this application. Stainless Steel was eliminated as a option due to problems maintaining structural integrity during construction of the fixed loop system. Titanium wire welded in a fixed loop was selected due to its low stretch under tension and the reliability and high strength during tension testing. Even with its small stretch under load, the straps still required pre stretching prior to installation to meet this application. Although the titanium straps have a higher thermal conductivity than the S-Glass Straps they represent a negligible parasitic impact to the canister as verified in thermal vacuum tests and in flight. The straps were installed in the BETSU and retested to protoflight levels without a failure.

The BETSU design caused significant difficulty to qualify the flight experiment. The following lessons learned are issues that should be considered when developing a cable tension system:

- Envelope Constraints:
The design should be user friendly and required a minimum effort for cable installation.
The tensioning method should be easily accessible and have ample travel.

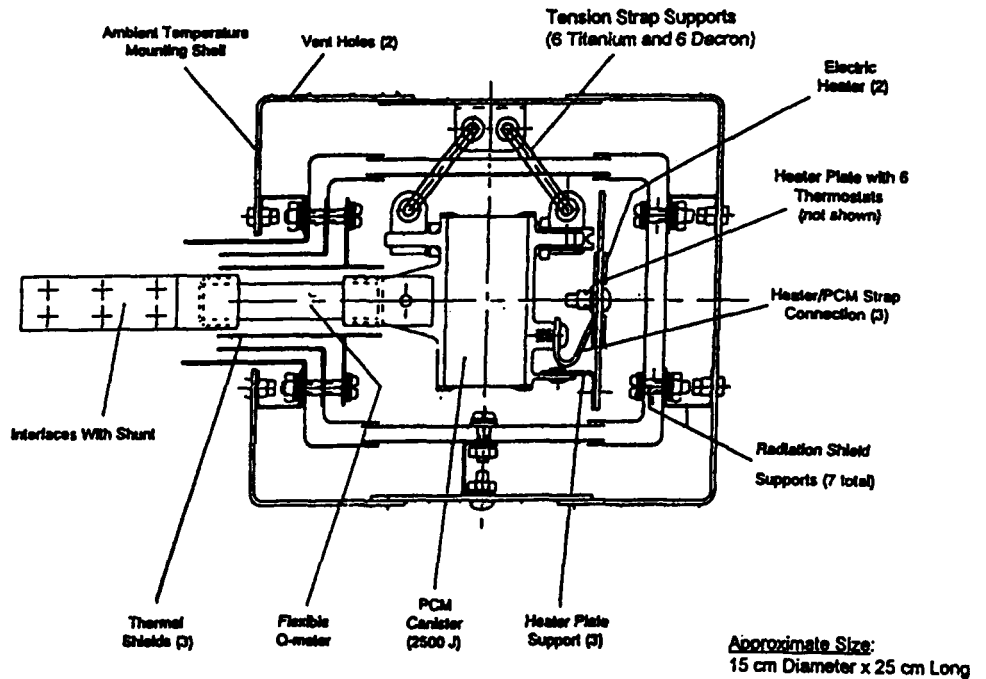


Figure 3. BETSU Structural Design

Table 1
CRYOTP Vibration Test Levels

Test #1 7-28-93			
Test	Input #1	Input #2	Outside Canister
Z-Axis Sine Burst	12.02	12.37	-2.24, -2, 15.15
Y-Axis Sine Burst	12.12	-12.44	-16.19, 3.67, -3.21
X-Axis Sine Burst	15.31	-14.19	-5.11, -19.21, 3.70
Z-Axis Random	5.523	4.105	7.92, 9.85, 12.12
Y-Axis Random	4.782	4.38	6.74, 6.84, 10.97
X-Axis Random	4.69	3.156	5.49, 4.90, 3.23

Allow access for inspection methods during qualification testing.

- **Short Cable Length:**
The length of the cable from centerline to centerline of the fixed ends should allow for stretch or give in cables.
- **Linear Take-up Mechanism:**
From our successful experience with the CTB heat pipe clamps we understand the benefit in having a mechanism to maintain tension under cable elongation. A spring type device, (convex washers) should be used in the tensioning mechanism to maintain tension of the cable when it elongates under load.

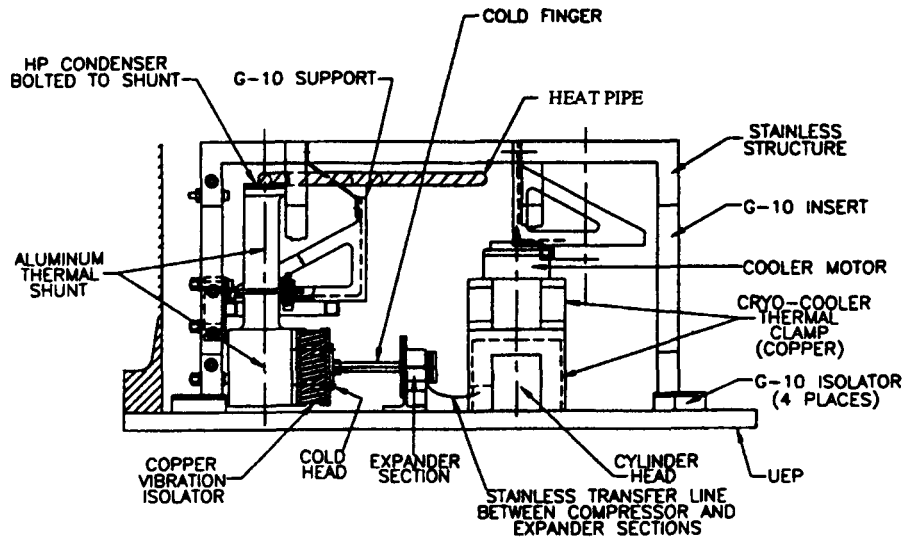


Figure 4. CTB Assembly

ARAMID CORD HEAT PIPE SUSPENSION

An aramid cord retention system was used as the primary means of support for the cryogenic heat pipes on the CRYOHP and CRYOTP flight experiments. This system was implemented to support the heat pipes during launch and landing loads and minimize the parasitic heat loads induced into the heat pipe. To fully understand the heat pipe support structure we will first describe the structural buildup to the heat pipes and then the heat pipe clamps themselves.

The rigid support of the UEP is transferred to the heat pipe location in the test bed by the heat pipe support structure (HPSS) as shown in Figure 4. This support structure is constructed of 19 mm (0.75") square stainless steel tubing welded in a truss structure with four base mounting pads. Thermal isolation between the UEP and the HPSS is provided by milled G-10 isolation pads between the mounting pads of the HPSS and the UEP and G-10 tubing inserts installed in the vertical legs of the HPSS. The HPSS is structurally attached by a fail safe attachment utilizing 1/4-20 hardware.

G-10 heat pipe support bodies shown in Figure 5 provide the rigid support for the cable attachment to the heat pipe and are attached to the HPSS by stainless steel hardware. The contact between the heat pipe support body and the HPSS is minimized by the low surface area of the body base in contact with the HPSS.

The cable attachment of the heat pipe is a wrap around method with locking pins to maintain tension in the required directions and a continuous load to keep the heat pipe from translating around its center line. Two parallel wrapped cables constructed of a 3 mm (0.12") diameter aramid weave are positioned perpendicular to the heat pipe, located 19 mm (0.75") apart forming a truss to the body attachment. The cable is installed by attaching the fixed end of the cable to the body and then wrapped around the heat pipe in the V-grooved rings epoxied to the heat pipe around the locking pins. The free end is brought through the body for tension screw attachment. Tension on the cable is adjusted by the tension screw located at the free end

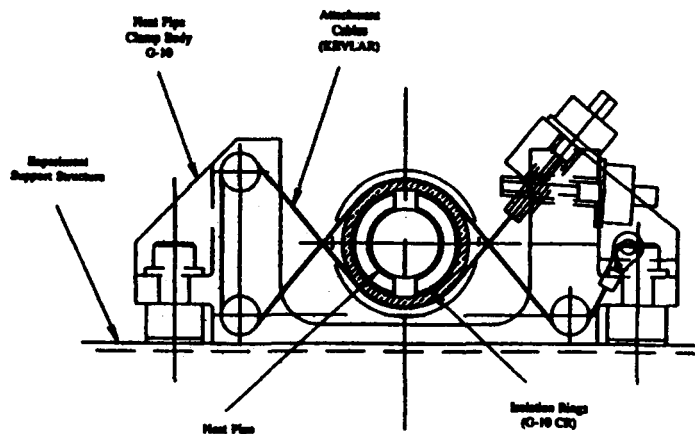


Figure 5. Heat Pipe Attachment and Isolation Support

of the cable. The tension setting for flight qualification is 25 lbs. Tension on the cable is maintained by self locking hardware between the body and the tension screw.

Two unexpected problems occurred during the development of the design:

- If the cable is continuous without locking at the pin locations the heat pipe could translate within the G-10 bodies.
- The tensioning system must have the ability to accommodate stretch in the cable due to the tension over time.

The continuous cable problem was eliminated by installing locking pins at the body pin locations and fixing the cable after final tensioning.

Accommodating the stretch in the cable due to tension over time was performed by using convex washers in the tension mechanism. The convex washers were stacked in an opposing orientation between the locking hardware of the tension screw and the heat pipe support bodies.

Course positioning of the heat pipe in the x-y coordinates of the experiment was accomplished by loosening the cables at the tension screws and physically locating the pipe at the correct level. The tension screw was then torqued to the proper tension and the cable was secured by tightening the locking pins. It is important to understand that the transitional stretch and adjustment of the cable is performed over time with periodic checks before locking down the pins. Fine elevation adjustment for the heat pipe is then provided by stainless steel shims between the HPSS and the heat pipe support body.

CRYO-COOLER VIBRATION ISOLATION MOUNT

The CTB flight experiments contained five tactical cryogenic split Stirling cycle coolers. These coolers were installed in the CTB experiments in the configuration as illustrated in Figure 6. The heat conductance and structural support coincide in this mounting configuration. The major portion of the heat is dissipated from the coolers in three locations: the compressor body, the cylinder head of the compressor, and the expander body. The compressor bodies and cylinder heads are heat sunk and rigidly mounted to the oversized, UEP by solid copper mounts on the three cooler side of the test bed and aluminum mounts on the two cooler side (aluminum was utilized to reduce mass and was possible due to the lower heat load 200 vs. 300 W) and the expander body is heat sunk and rigidly mounted to the UEP by gold plated mounts. All body mounting locations used graphite foil as a thermal interface material. The coolers are configured on the UEP as illustrated in Figure 6. This configuration optimizes the amount of coolers and provides two independent test beds.

These coolers produce a vibration due to their internal working system. As illustrated in Figure 7 the vibration induced from the coolers originates from three locations in the system; the

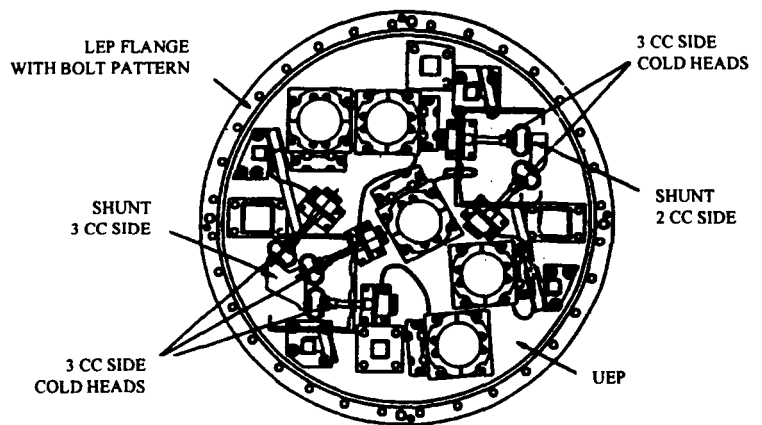


Figure 6. CTB Cry-Cooler Configuration

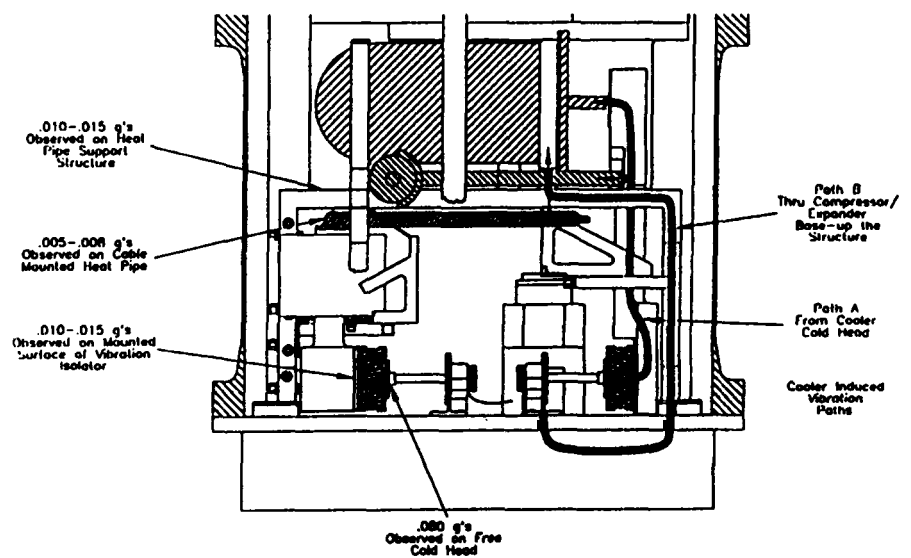


Figure 7. CTB Cry-Cooler Induced Vibration

compressor body, the expander body and the cold head of the expander. The expander and compressor bodies were hard mounted to the UEP and vibration loads are transmitted up to the experiment area through the heat pipe support structure. The majority of the vibration is induced by the piston in the expander tube and is applied at the cold head of the coolers. This induced vibration is translated directly to the test articles through the thermal shunt.

During the development of the mounts, tests were performed to characterize the vibration induced at the cold head of the coolers. A cooler was mounted on the UEP in the flight configuration. The base of the compressor and expander bodies were rigidly mounted with graphite foil between the interface to reflect the flight configuration. This test set-up was fully instrumented providing vibration readings across the UEP and on the cold head of the cooler. The most severe vibration was emitted in line with the expansion tube perpendicular to the cold head having a magnitude of approximate 80 milli-g's. The result was consistent across the several tests performed.

The development of the vibration isolation system between the cold head and the experiment interface required a design study to evaluate the following parameters:

- thermal conductance
- vibration isolation
- load, induced on the cold head
- envelope available
- cost

The design team developed a simple copper braided vibration isolation mount to be mounted between the individual cold plate head of the coolers and the thermal shunt. This thermally conductive vibration isolator is constructed of copper braid sandwiched between two copper plates at each end. Epoxy was used to bond the copper plates with the braid.

Tests were run with full instrumentation mapping the test bed including a sample heat pipe. The results of the total assembly are illustrated in Figure 7. The resulting conductance across the mounts was approximately 2 W/°C and the mounts in the configuration of the test bed reduced the vibration across the isolation mounts to .010-.015 milli-g's and at the heat pipe to .005 to .008 - Milli-g's.

It is important to understand the test bed configuration, the oversized UEP and aramid cable heat pipe mount in combination with the vibration isolators, achieved the results.

CRYOHP (CTB I)

The first flight of the CTB tested two axially grooved oxygen heat pipes. Heat Pipe #1 was 11.2 mm in diameter and had a special groove geometry that was intentionally degraded so that its transport capacity could be tested within the limits of the CTB's cooling capacity (~ 5 watts net at 80 K). Heat Pipe #2 was 15.9 mm in diameter and had a transport capacity that exceeded the capacity of the CTB permitting demonstration of priming from the super critical state and transport but not transport limit verification or recovery demonstration.. These heat pipes provided the first available flight data

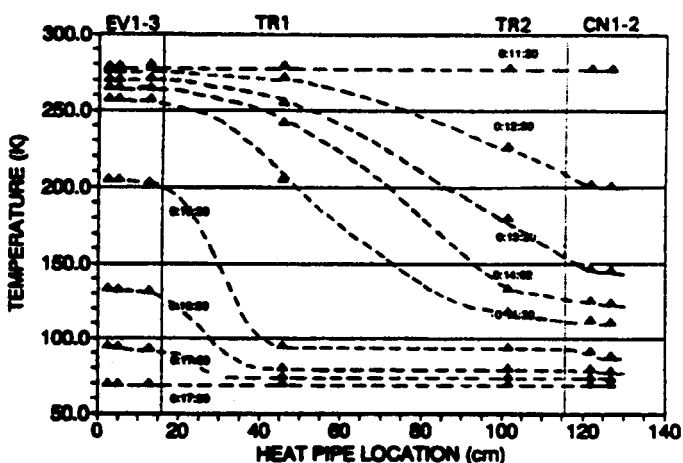
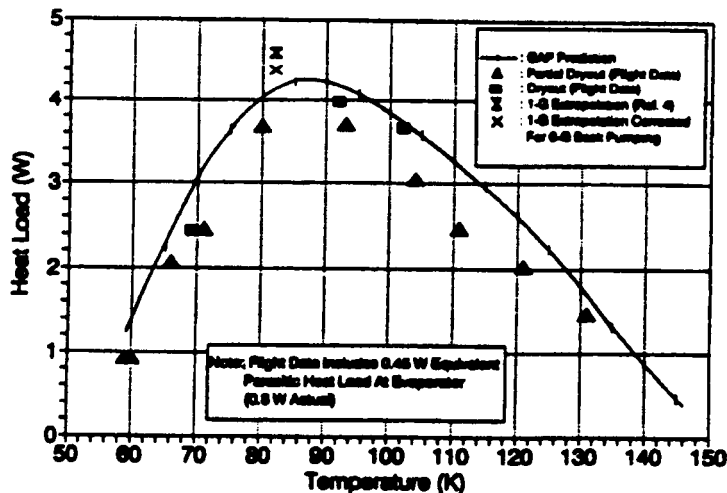


Figure 8. Axial Profile of Heat Pipe #1 Transient Cooldown



"As-Fabricated" Groove Dimensions for GAP Predictions:
 $D_o=11.22$ mm $D_i=8.87$ mm $D_v=7.28$ mm 17 Grooves
 $W_g=0.445$ mm $W_p=2.08$ mm $R_t=0.102$ mm $A_g=8.07$ mm²

Figure 9. Heat Pipe #1 Transport Capability

for cryogenic heat pipes that operate below 100 K.

Heat Pipe #1

The first cooldown of Heat Pipe #1 started at mission elapsed time (MET) 11:22. Figure 8 shows the axial temperature profile for the first transient cooldown of Heat Pipe #1. The cooldown took approximately 6 hours. The heat pipe condenser was cooled to the critical point of oxygen in two hours marking the beginning of condensation. The cooldown was performed three times and all were essentially identical. Figure 9 compares the flight performance of the heat pipe with the pre-flight ground testing. The flight data has been adjusted by an equivalent 0.45 watts evaporator heat load to adjust for a 0.8 watt parasitic heat load. The flight data is in reasonably good agreement with the groove analysis program (GAP) predictions. The flight performance is consistently 0.4 to 0.6 watts below the GAP predictions which was used to improve the model.

Heat Pipe #2

The first cooldown of Heat Pipe #2 started at MET 22:18. Figure 10 shows the axial temperature profile for the first transient cooldown of Heat Pipe #2. The cooldown took approximately 6.5 hours, the increased time compared to Heat Pipe #1 is due to decreased cooling capacity of the two cooler side of the experiment. The heat pipe condenser was cooled to the critical point of oxygen in 3.25 hours marking the beginning of condensation. The cooldown was performed twice and both were essentially identical. Figure 11 compares the flight performance of the heat pipe with the pre-flight ground testing. The flight data has been adjusted by an equivalent 0.64 watts evaporator heat load to adjust for a 1.14 watt parasitic heat load. The flight data is in good agreement with the GAP predictions.

We attempted a third flight cool down of the heat pipe however the cryo-coolers did not perform well. The UEP was at 332 K (59°C) when we turned them on and the cold heads were at 277 K (4°C). Post flight testing and discussions with the manufacturer has led us to believe that the high cooler temperatures had driven all system moisture to the cooler cold heads where it froze when the cold heads reached 0°C. The units had fully recovered after time and performed nominally during post flight testing.

CRYOTP (CTB II)

The second flight of the CTB tested the BETSU and a nitrogen heat pipe (NHP). The BETSU is a phase change material (PCM) canister using 35 grams of

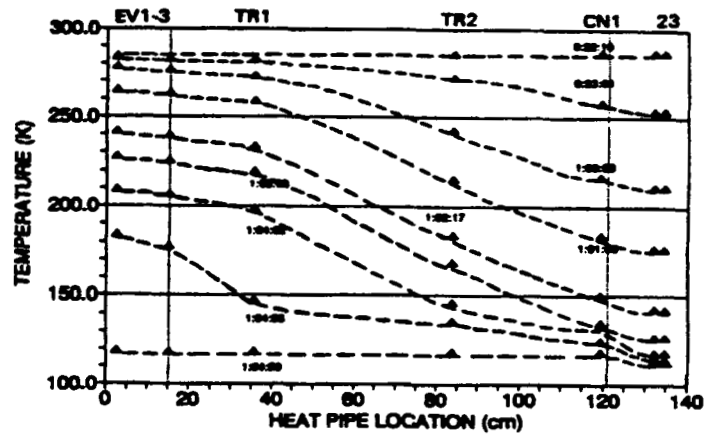


Figure 10. Axial Profile of Heat Pipe #2 Transient Cooldown

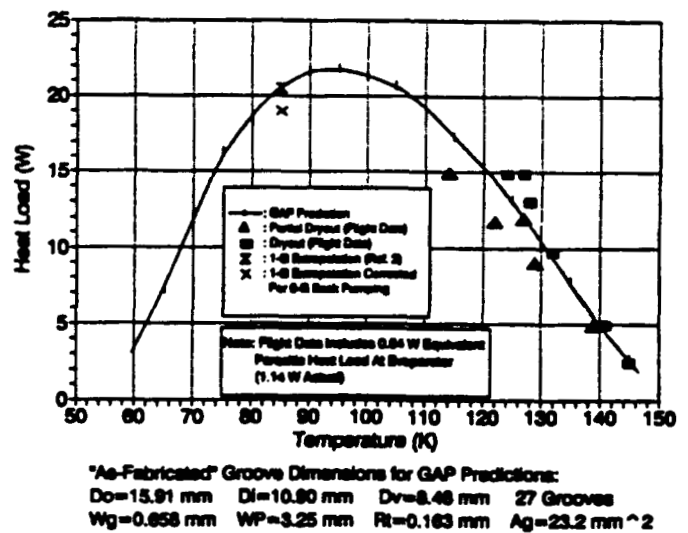


Figure 11. Heat Pipe #2 Transport Capability (PCM Hot Side)

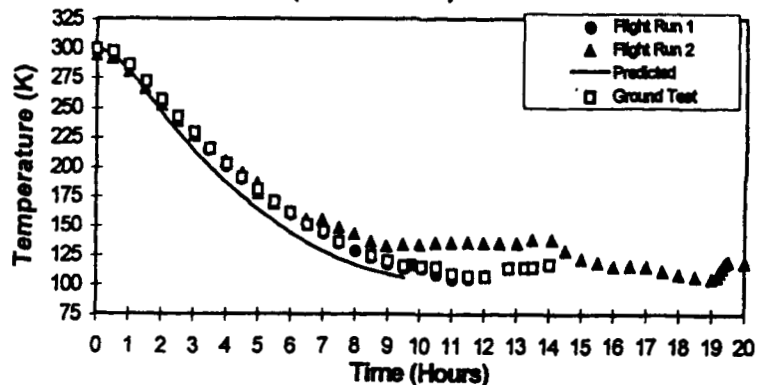


Figure 12. Comparison of BETSU Ground and Flight Transient Cooldowns

2-methylpentane with 3% acetone added. The BETSU provides 2500 Joules of energy storage with a freeze/thaw point at 120 K. The NHP was fabricated from titanium - Ti-6Al-4V (ELI), has a 15 mm diameter and is charged with 24.1 grams of nitrogen.

BETSU

The assembly of the BETSU is shown in Figure 3. The first BETSU cooldown started approximately 23 hours MET. Figure 12 presents the cooldown data for two flight cycles and compares them to ground and predicted data. On the first cooldown cycle the PCM did not freeze until it was cooled to 105 K and the temperature climbed to 117.5 K as the heat of fusion was released. The second cycle was nearly the same with supercooling occurring at 105.4 K and freezing at 119.8 K. More than 200 hours of on-orbit data consisting of fifty-five freeze/thaw cycles and 26 steady state calibrations were completed. Results from ground and flight tests show that virtually all of the stored energy (2472 J) is realized during the phase cycling. Temperature control at 119 ± 1.5 K was demonstrated with a one watt heating rate.

NHP

The cooldown of the NHP was initiated within minutes of CRYOTP turn on. Figure 13 shows the axial profile of the transient cool down. A second cycle was performed on day 6 of the mission. The NHP did not isothermalize in either cycle. Both cycles had similar cool down profiles. The anomaly was initially attributed to an excessive liquid slug, however, further analysis has been performed and a paper was presented on this topic at the International Heat Pipe Conference in Albuquerque in 1995. That paper points to design issues that need to be addressed when designing cryogenic heat pipes to prevent the anomaly that the NHP demonstrated on orbit.

CRYOFD (CTB III)

The third flight of the CTB will test two cryogenic flexible diode heat pipes. One heat pipe will be an oxygen pipe and the other will be charge with methane. The oxygen heat pipe will be tested over the temperature range of 60 - 100 K and the methane heat pipe will have a nominal operating temperature of 120 K. The flexible nature of the CFDHPs

will allow for differential thermal contraction and expansion for large temperature gradients and dissimilar materials. The diode operation will isolate an instrument from redundant (or failed) cryo-coolers, or a hot radiator.

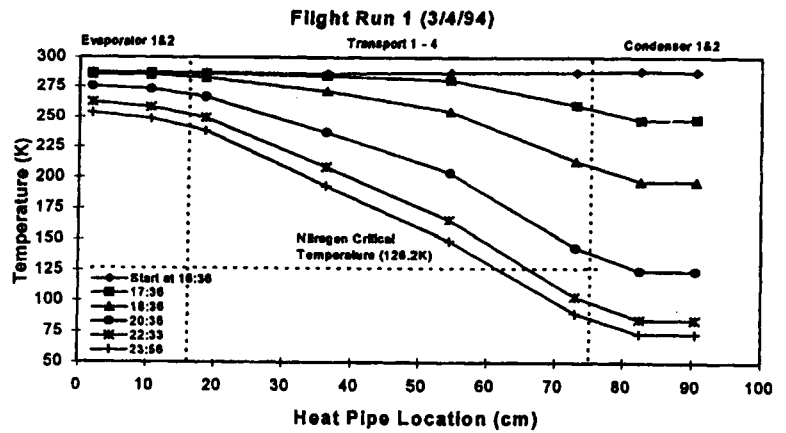


Figure 13. Axial Profile of NHP Cooldown

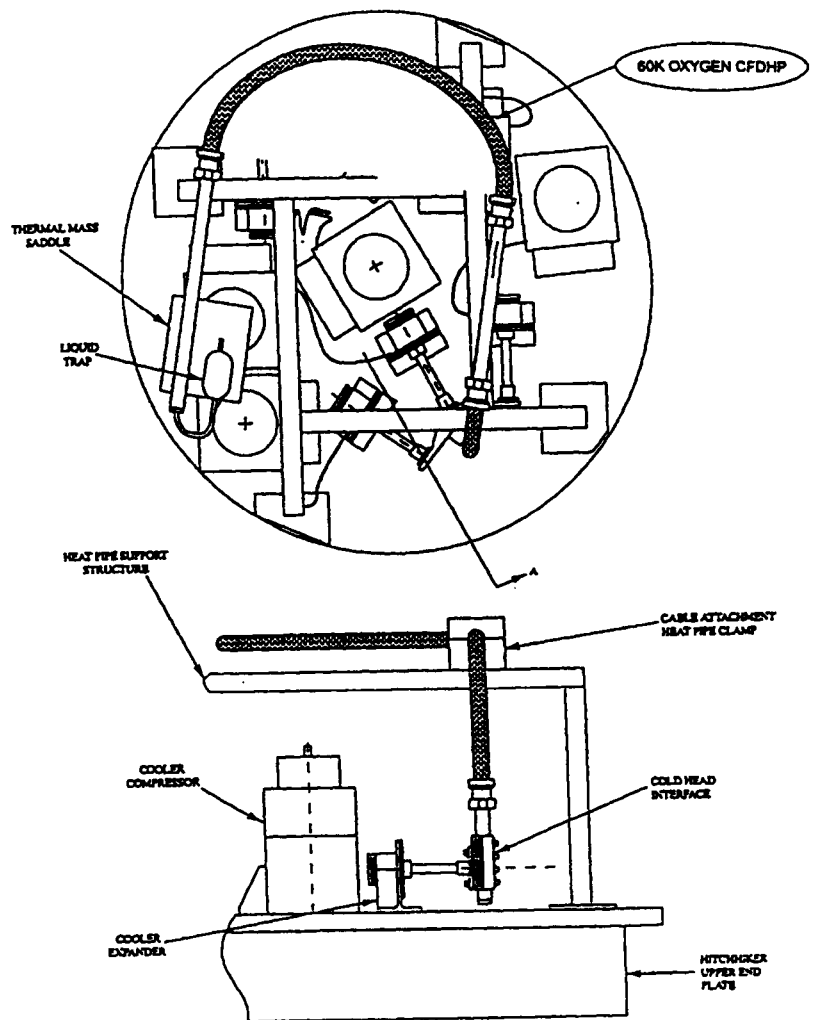


Figure 14. CRYOFD Configuration

Acronyms:

BETSU	Brilliant Eyes Thermal Storage Unit	IVT	Interface Verification Test
CECM	CTB Electronics Control Module	JSC	Johnson Space Center
CoP	Coefficient of Performance	K	Kelvin(s)
CRYOFD	Cryogenic Flexible Diode Experiment	LEP	Lower End Plate (of a HH canister)
CRYOHP	Cryogenic Heat Pipe Experiment	LN ₂	Liquid Nitrogen
CRYOTP	Cryogenic Two Phase Experiment	MET	Mission Elapsed Time
CTB	Cryogenic Test Bed	MLI	Multi Layer Insulation
EMC	Electromagnetic Compatibility	NHP	Nitrogen Heat Pipe
EMI	Electromagnetic Interference	NSTS	National Space Transportation System
GAP	Groove Analysis Program	PCM	Phase Change Material
GSE	Ground Support Equipment	PDB	Power Distribution Box
GSFC	Goddard Space Flight Center	PRT	Platinum Resistance Thermometer
HH	Hitchhiker	UEP	Upper End Plate
HPSS	Heat Pipe Support Structure		

References:

1. Brennan, P., Stouffer, C., Thienel, L., and Morgan, M., "Performance of the Cryogenic Heat Pipe Flight Experiment" SAE Technical Paper Series number 921408, July 1992.
2. Brennan, P., Thienel, L., Swanson, T., and Morgan, M., "Flight Data for the Cryogenic Heat Pipe (CRYOHP) Experiment" AIAA Paper number 93-2735, July 1993.
3. Brennan, P., Thienel, L., Stoyanof, M., Bello, M., "Design and Performance of the Cryogenic Two Phase Flight Experiment" SAE Technical Paper Series number 941474, June 1994.
4. Brennan, P., Thienel, L., "Cryogenic Heat Pipe Technology" NASA/GSFC Capillary Pumped Loop Workshop IV, September 1994.
5. Thienel, L., Stouffer, C., Brennan, P., "The Cryogenic Test Bed, A Discussion of Techniques Used and Lessons Learned Through Two Shuttle Flights (STS-53 and STS-62)" 1st Annual Spacecraft Thermal Control Symposium, 16 - 18 November 1994, Albuquerque, New Mexico.